水果受衝擊時之動態分析

Dynamic Analysis of Fruit Impact

國立臺灣大學農機系副教授

陳　世　銘

Suming Chen

摘　要

水果在收穫及收穫後的機械作業時，常因碰撞和衝擊而受傷。爲了減少損傷，維持水果品質，並提供設計收穫及加工機械的有用資料，水果衝擊的研究有其實用價值上的重要性。本研究已成功地完成動態有限元素分析數學模型的建立，並寫成電腦程式。這個模型可以用來分析水果在受衝擊時，水果內部應變和應力的分佈情況，並可以預測水果內部各點的速度和加速度之變化情形。本模型是將水果視爲軸對稱的物體，並假設在剪力方向的反應爲線性黏彈性反應，在容積上爲彈性反應。本模型的動態分析是採用Wilson-θ方法，其中θ的值爲 1.4，並經實驗驗證無誤。本研究結果亦與文獻資料相互驗證，並作比較，能以動態進行分析爲本模式最大之特點。

關鍵詞：動態、衝擊、水果、有限元素法

ABSTRACT

During harvesting and subsequent handling, fruits are subjected to impact situations which often cause bruises and injuries. The study of fruit impacts has practical significance in that useful information can be provided for the proper design of harvesting and handling equipment to minimize injury and to maintain the quality of fruits. A dynamic finite element procedure and computer program were successfully developed to analyze the stress-strain and velocity-acceleration distributions within the fruit under impact situations. The fruit was treated as an axisymmetric body and was assumed to exhibit a linear viscoelastic response in shear and an elastic response in bulk. The Wilson-θ method with θ=1.4 was used in this dynamic analysis. The model was experimentally verified. Numerical results were also compared with those reported by other researchers, and the dynamic analysis was the key feature of this model.

Keywords: Dynamic, Impact, Fruits, Finite Element Method

Introduction

During harvesting and handling, fruits are subjected to impacts which often cause bruises and injuries. Since fruits are known to behave viscoelastically, the study of responses of viscoelastic materials to impacts provides useful information for designing harvesting and handling equipment to minimize injury and maintain the quality of the fruit.

Timoshenko and Goodier (1951) extended Hertz's contact theory and derived equations for impact of two elastic spheres. Timoshenko and Goodier's elastic-impact theory was extended by Horsfield et al. (1972) to determine the maximum internal shear stress of fruit impact. Hamann (1970) modified Yang's (1966) viscoelastic-contact theory to allow the calculation of internal stresses in the impacting body. His scheme was based on rigid-body motion and a quasi-static assumption. Herrmann and Peterson (1968) developed a finite element procedure for a static viscoelastic stress analysis for 2-D solids, which provides a relatively easy method for internal stress calculations. Rumsey and Fridley (1977) modified Herrmann's finite-element procedure to include the consideration of contact and impact. The impact loading was simulated by moving a rigid plate onto the top of the sphere. The displacement boundary condition of contact nodes was introduced by using the ridig-body impulse-momentum law.

Since impact of fruits is a dynamic process, any theory based on quasi-static assumptions is theoretically inaccurate. Nevertheless, analysis with quasi-static assumpions can provide results acceptable for practical use.

In this study, a dynamic finite-element procedure was developed to analyze the stress distribution within the fruit under impact. The fruit was treated as a 2-D, axisymmetric body linear-viscoelastic in shear and elastic in bulk. Impact of fruit on a rigid plate was investigated by assigning a velocity and acceleration to each node of the apple as initial conditions before impact (Chen, 1985). The consideration of inertial effect for each node (interior and boundary) allows more accurate predictions of stress distribution within fruit during impact than is possible by quasi-static means.

Theory

Stress-Strain Law

The total stress, τ_{ij}, and strain, ε_{ij}, tensors can be separated into deviatoric components, s_{ij} and e_{ij}, and volumetric components, σ and θ, as follows:

$$s_{ij} = \tau_{ij} - \sigma \delta_{ij} \qquad [1]$$

$$e_{ij} = \varepsilon_{ij} - \frac{\theta}{3} \delta_{ij} \qquad [2]$$

$$\sigma = \frac{1}{3} \sum_{i=1}^{3} \tau_{ii} \qquad [3]$$

$$\theta = \sum_{i=1}^{3} \varepsilon_{ii} \qquad [4]$$

where

$$\delta_{ij} = \begin{cases} 0, & i \neq j \\ 1, & i = j \end{cases} \qquad [5]$$

For linear isotropic viscoelastic materials, s_{ij} and σ can be expressed by the following expressions (Moreland and Lee, 1960):

$$s_{ij} = 2 \int_{o}^{t} \phi_1 (t-\tau) \frac{\partial e_{ij}}{\partial \tau} d\tau \qquad [6]$$

$$\sigma = \int_o^t \phi_2 (t-\tau) \frac{\partial \theta}{\partial \tau} d\tau \qquad [7]$$

where ϕ_1 and ϕ_2 are relaxation functions in shear and bulk, respectively.

As a comparison, for linear isotropic elastic materials

$$s_{ij} = 2\mu e_{ij} \qquad [8]$$

$$\sigma = k\theta \qquad [9]$$

where μ and k are the elastic shear modulus and the elastic bulk modulus, respectively.

For our model we assumed that the fruit is viscoelastic in shear and elastic in bulk; therefore, equations [6] and [7] become

$$s_{ij} = 2\int_0^t \phi_1 (t-\tau) \frac{\partial e_{ij}}{\partial \tau} d\tau \qquad [10]$$

$$\sigma = k\theta \qquad [11]$$

The shear relaxation function, ϕ_1, can be expressed in the following form:

$$\phi_1(t) = \sum_{m=1}^{M} G_m e^{-\beta_m t} \qquad [12]$$

Substituting equation [12] into equation [10] and performing an incremental analysis, equations [10] and [11] are transformed into the following:

$$\Delta s_{ij_n} = 2\mu_n \Delta e_{ij_n} + s_{ijo_n} \qquad [13]$$

$$\Delta\sigma_n = k\Delta\theta_n \qquad [14]$$

where,

$$\Delta s_{ij_n} = s_{ij_n} - s_{ij_{n-1}} \qquad [15]$$

$$\Delta e_{ij_n} = e_{ij_n} - e_{ij_{n-1}} \qquad [17]$$

$$\Delta\sigma_n = \sigma_n - \sigma_{n-1} \qquad [18]$$

$$\Delta\theta_n = \theta_n - \theta_{n-1} \qquad [19]$$

$$\Delta t_n = t_n - t_{n-1} \qquad [20]$$

$$\mu_n = \sum_{m=1}^{M} G_m J_{m_n} \qquad [21]$$

$$J_{m_n} = \frac{1}{\beta_m \Delta t_n} [1 - e^{-\beta_m \Delta t_n}] \qquad [22]$$

$$s_{ijo_n} = 2 \sum_{m=1}^{M} G_m [e^{-\beta_m \Delta t_n} - 1] C_{ijm_n} \qquad [23]$$

$$C_{ijm_n} = e^{-\beta_m \Delta t_{n-1}} C_{ijm_{n-1}} + \Delta e_{ij_{n-1}} J_{m_{n-1}} \qquad [24]$$

In equations [13] and [14], the incremental shear modulus, μ_n, is a time dependent property, whereas the elastic bulk modulus, k, is a constant. The history effect resulting from viscoelasticity is introduced by the term s_{ijo_n}.

Dynamical Analysis

By using the stress-strain law and the theorem of minimum potential energy and considering inertial forces, the system matrix equation of the finite-element procedure can be expressed as (Bathe, 1982)

$$\underset{\approx}{M}\,\underset{\sim}{\ddot{U}} + \underset{\approx}{S}\,\underset{\sim}{U} = \underset{\sim}{R} \qquad [25]$$

where $\underset{\approx}{M}$ and $\underset{\approx}{S}$ are system-mass and system-stiffness matrices, respectively, $\underset{\sim}{\ddot{U}}$, $\underset{\sim}{U}$ and $\underset{\sim}{R}$ are system acceleration, dis-

placement and load vectors, respectively. Note that $\underset{\approx}{S}$ is function of time.

For time interval t to t + Δt, assume $\underset{\approx}{M}$ and $\underset{\approx}{S}$ remain constant. Then

$$\underset{\approx}{M}_t \Delta\ddot{\underset{\sim}{U}}_{t+\Delta t} + \underset{\approx}{S}_t \Delta\underset{\sim}{U}_{t+\Delta t} = \Delta\underset{\sim}{R}_{t+\Delta t} \quad [26]$$

where

$$\Delta\ddot{\underset{\sim}{U}}_{t+\Delta t} = \ddot{\underset{\sim}{U}}_{t+t\Delta t} - \ddot{\underset{\sim}{U}}_t \quad [27]$$

$$\Delta\underset{\sim}{U}_{t+\Delta t} = \underset{\sim}{U}_{t+t\Delta t} - \underset{\sim}{U}_t \quad [28]$$

$$\Delta\underset{\sim}{R}_{t+\Delta t} = \underset{\sim}{R}_{t+\Delta t} - \underset{\sim}{R}_t \quad [29]$$

The element mass matrix, $\underset{\approx}{M}^{(e)}_{ij}$, can be expressed as (Zienkiewicz, 1977)

$$\underset{\approx}{M}^{(e)}_{ij} = \int_{v^{(e)}} \underset{\sim}{N}^T \rho \, \underset{\sim}{N} \, dv \quad [30]$$

where $\underset{\sim}{N}$ is a shape function and ρ is the material density.

For a constant-density axisymmetric body using quadrilateral elements in the finite-element analysis

$$\underset{\approx}{M}^{(e)} = \rho \int_{v^{(e)}} \underset{\sim}{N}^T \underset{\sim}{N} (rdrdzd\theta) \quad [31]$$

By considering only a unit radian and transforming coordinates r and z to master element coordinates ξ and η, equation [31] becomes,

$$\underset{\approx}{M}^{(e)} = \rho \int_{-1}^{1} \int_{-1}^{1} \underset{\sim}{N}^T \underset{\sim}{N} (\Sigma R_i N_i) \, |J| \, d\xi d\eta \quad [32]$$

Where R_i = nodal r-coordinates

|J| = Jacobian

$$N_i = \frac{1}{4}(1 + \xi_i \xi)(1 + \eta_i \eta) \quad [33]$$

As pointed out by Zienkiewicz (1977), the results of analyses using consistent-mass and lumped-mass matrices are almost identical in practice. For simplicity, the lumped-mass procedure is applied to equation [32].

The Wilson-θ method (Bathe and Wilson, 1976) is used to solve equation [26]. This method is basically an extension of the linear-acceleration method; it does not need a special starting procedure, and is an implicit method with unconditional stability if $\theta \geqslant 1.37$. In practice, the value of θ is usually set at 1.4 (Lapidus and Pinder, 1982).

After an incremental analysis with the Wilson-θ method, equation [26] becomes

$$\tilde{\underset{\approx}{S}}_{t+\theta\Delta t} \Delta\underset{\sim}{U}_{t+\theta\Delta t} = \Delta\tilde{\underset{\sim}{R}}_{t+\theta\Delta t} \quad [34]$$

where,

$$\tilde{\underset{\approx}{S}}_{t+\theta\Delta t} = \underset{\approx}{S}_t + \frac{6}{(\theta\Delta t)^2} \underset{\approx}{M}_t \quad [35]$$

$$\Delta\tilde{\underset{\sim}{R}}_{t+\theta\Delta t} = \theta\Delta\underset{\sim}{R}_{t+\Delta t} + \underset{\approx}{M}_t \left[\frac{6}{\theta\Delta t} \dot{\underset{\sim}{U}}_t + 3\ddot{\underset{\sim}{U}}_t \right] \quad [36]$$

where $\tilde{\underset{\approx}{S}}_{t+\theta\Delta t}$ is effective system stiffness matrix and $\Delta\tilde{\underset{\approx}{R}}_{t+\theta\Delta t}$ the is effective system incremental load vector. The changes in displacement, velocity, and acceleration for the time interval, Δt, can then be expressed as

$$\Delta\ddot{\underset{\sim}{U}}_{t+\Delta t} = \left[\frac{6}{(\theta\Delta t)^2} \Delta\underset{\sim}{U}_{t+\theta\Delta t} - \frac{6}{\theta\Delta t} \dot{\underset{\sim}{U}}_t - 3\ddot{\underset{\sim}{U}}_t \right] / \theta \quad [37]$$

$$\Delta\dot{\underset{\sim}{U}}_{t+\Delta t} = \ddot{\underset{\sim}{U}}_t \Delta t + \frac{\Delta t}{2} \Delta\ddot{\underset{\sim}{U}}_{t+\Delta t} \quad [38]$$

$$\Delta\underset{\sim}{U}_{t+\Delta t} = \dot{\underset{\sim}{U}}_t \Delta t + \frac{(\Delta t)^2}{2} \ddot{\underset{\sim}{U}}_t + \frac{(\Delta t)^2}{6}$$

$$\Delta\ddot{\underset{\sim}{U}}_{t+\Delta t} \quad [39]$$

finally

$$\underset{\sim}{U}_{t+\Delta t} = \underset{\sim}{U}_t + \Delta\underset{\sim}{U}_{t+\Delta t} \quad [40]$$

$$\dot{\underset{\sim}{U}}_{t+\Delta t} = \dot{\underset{\sim}{U}}_t + \Delta\dot{\underset{\sim}{U}}_{t+\Delta t} \quad [41]$$

$$\ddot{\underset{\sim}{U}}_{t+\Delta t} = \ddot{\underset{\sim}{U}}_t + \Delta\ddot{\underset{\sim}{U}}_{t+\Delta t} \quad [42]$$

Numerical Procedure

A finite-element program was developed to include the inertial effect by modifying a static-viscoelastic-analysis program for 2-D solids (Herrmann, 1973). The Wilson-θ method was used for this modification. This numerical procedure for dynamic analysis was verified by comparison to an analytic solution of wave propagation in an elastic half-space subjected to uniform surface tractions. The results of the two methods showed excellent agreement in both normal stress and particle-velocity values (Chen, 1985).

The procedure was further modified to handle contact between the viscoelastic body and a rigid surface. The position of the rigid surface is fixed and serves as a reference position to determine whether any new exterior-boundary nodes on the fruit are in contact with the rigid surface. Once a new boundary node contacts this surface, an adjusted-displacement boundary condition is assigned to this node, and an iteration of the same time increment is introduced. The acceleration, velocity and incremental displacement are all set to zero for the contact nodes for the rest of the time increments. Maximum deformation of the fruit is reached when the velocity of the non-contact node nearest to the contact nodes changes direction.

Results and Discussion

The fruit was initially assumed to be a sphere, which then remained axisymmetric under impact loadings. Therefore, only a half circle domain was needed for finite-element calculations. Several grid patterns and mesh sizes were examined. A grid with 88 elements and 106 nodes (Fig. 1) was selected because this grid

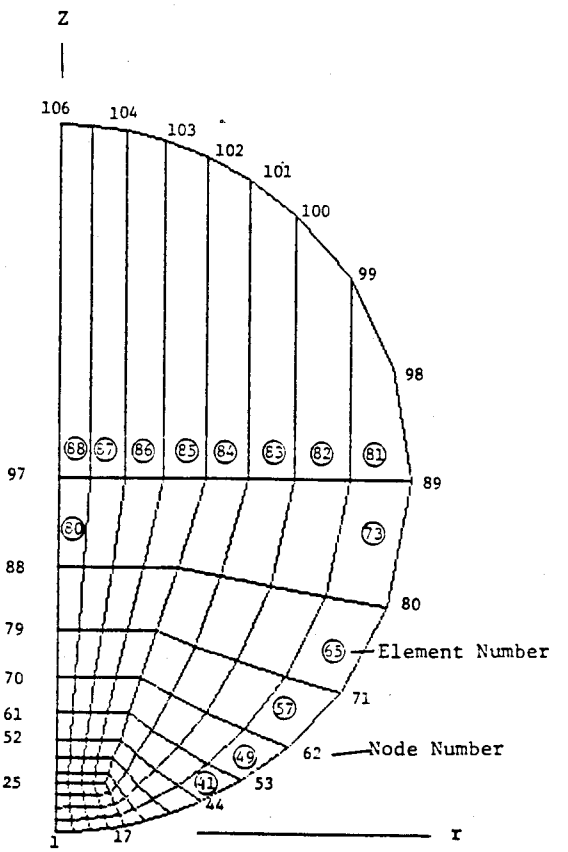

Fig. 1 Finite element grid of apple section with grid pattern of 88 elements and 106 nodes.

configuration gave good accuracy at low computing cost.

Experimental Verification

The dynamic finite element procedure was further verified by the experimental measurements of acceleration at the center of the fruit. The instrument design and experimental procedure have been discussed by Chen (1985) and Chen et al. (1985). These comparison are shown in Figure 2 for Golden Delicious apples and a drop height of 25.4 mm. The excellent agreement once again confirms the validity of dynamic finite element procedure. The grid with 88 elements and a time increment of 0.02 ms were used for the finite element calculations.

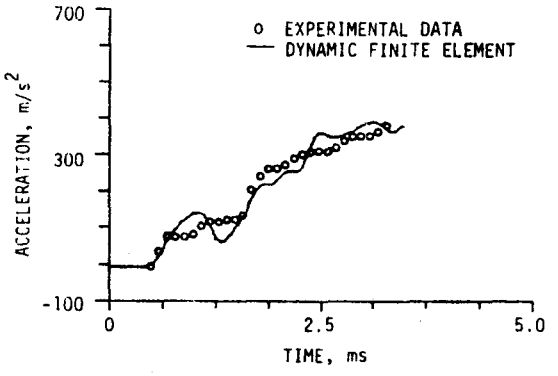

Fig. 2. Verification of dynamic finite element procedure by experiemental measurements of acceleration at the center of a Golden Delicious apple for a drop height of 25.4 mm

Elastic Impact

The finite element program can also handle elastic problems. For the purpose of verifying the program, the problem of impact of an elastic sphere on a rigid plate after a 0.05-m drop was investigated. The results of this dynamic analysis were compared with the theory of elastic impact by Timoshenko and Goodier (1951) and with the elastic-impact results of Rumsey and Fridley (1977).

Timoshenko and Goodier gave the maximum deformation, α_m, time at α_m, t_m, and maximum surface pressure, q_m, as

$$\alpha_m = \left(\frac{15(1-\nu^2)MV^2}{16\,E\sqrt{R}} \right)^{0.4} \qquad [43]$$

$$t_m = \frac{1.47\alpha_m}{V} \qquad [44]$$

$$q_m = \frac{2E}{\pi(1-\nu^2)} \sqrt{\frac{\alpha_m}{R}} \qquad [45]$$

where

V = initial velocity of sphere at impact,

ν = Poisson's ratio,

E = Young's modulus,

M = mass of sphere,

R = radius of sphere.

Comparison of α_m, t_m, and q_m for each of the three methods was made using the following material properties and conditions:

V = 0.9982 m/s

ν = 0.219

E = 18.11 MPa

M = 0.155 Kg

R = 0.0366 m

Table 1. Comparisons of maximum deformation, time required to reach maximum deformation, and maximum surface pressure for elastic impacts.

Method	Maximum Deformation, α_m mm	Time to reach α_m ms	Max. surface pressure, q_m MPa
*Dynamic finite-element	1.096	1.51	1.99
Rumsey and Fridley	1.107	1.60	2.19
Timoshenko & Goodier	1.097	1.62	2.10

*Time increment used = 0.01 ms

$\ddot{U} = 9.8$ m/s^2 (initial acceleration)

$\rho = 756.85$ Kg/m^3 (density of fruit)

Comparisons of α_m, t_m, and q_m are shown in Table 1. The dynamic finite-element procedure predicted a lower surface pressure than those of other methods. The differences are very small in maximum deformation predicted by the three methods (1%), but the dynamic finite-element analysis predicts a shorter time to reach maximum deformation than the other methods.

The deformation and maximum surface pressure curves are compared in Figures 3 and 4 where Goldsmith's (1960) approximate equation,

$$\alpha(t) = \alpha_m \sin\left(\frac{1.068\ Vt}{\alpha_m}\right), \qquad [46]$$

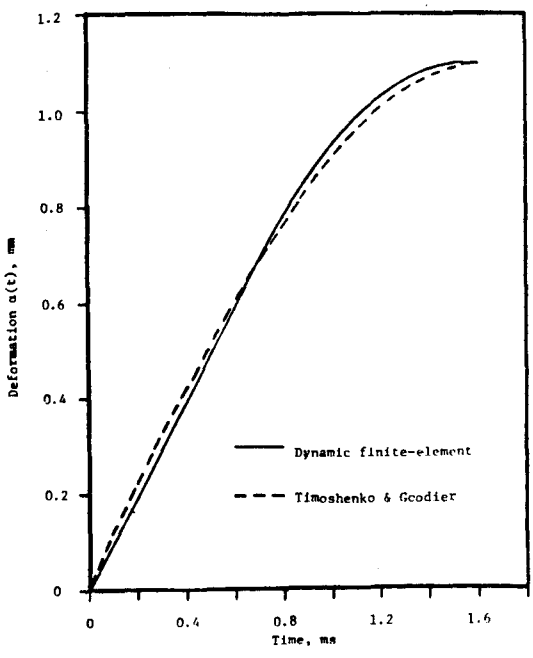

Fig. 3. Comparison of deformation curves for elastic impact on a rigid plate.

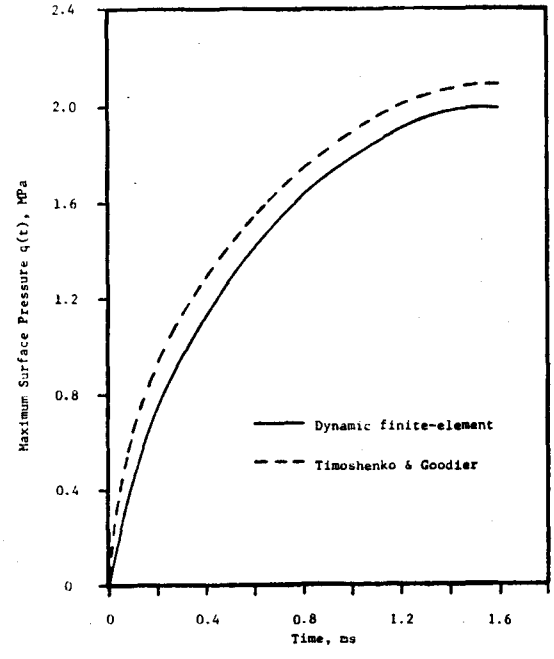

Fig. 4. Comparison of maximum surface-pressure curves for elastic impact on a rigid plate.

is used for Timoshenko and Goodier's theory.

The maximum deformation and maximum surface pressure occur at the same time for both dynamic and the quasi-static solutions for elastic impact.

Viscoelastic Impact

The results of viscoelastic impact determined with the dynamic finite-element analysis were compared with those obtained by Rumsey and Fridley (1977) and Hamann (1970). For making comparisons, the material properties derived by Rumsey and Fridley (1977) and Hamann (1970) were used. A comparison with results by Rumsey and by Hamann is listed in Table 2 for a 0.05-m drop of a viscoelastic sphere, with radius of 0.0366 m and density of 757 kg/m^3, onto a rigid plate. In all three methods, the maximum surface pressure occurs earlier than the maximum deformation does. But, as in the case of elastic impact, the dynamic finite-element procedure predicts lower maximum surface pressure. The time required to reach maximum deformation is the same for the quasi-static methods but is shorter for the dynamic finite-element procedure.

The material properties at impact or high-strain-rate conditions were not the same as under static or quasi-static conditions. Work has been done by Chen and Chen (1986) to determine dynamic material properties.

The uniaxial relaxation stress, $\sigma(t)$, resulting from a step strain input can be expressed by a Maxwell model as

$$\sigma(t) = \sum_{i=1}^{n} \varepsilon_o E_i e^{-\alpha_i t} \qquad [47]$$

where E_i and α_i are constants, ε_o is a constant uniaxial strain, and t is time.

The stress and strain analysis for viscoelastic materials by the finite-ement procedure requires knowledge of the shear relaxation function, ϕ_1, (equation [10]). The shear relaxation function, ϕ_1, can be obtained from equation [47], and its Laplace transform is expressed by Rumsey and Fridley, (1977) as

Table 2. Comparisons of maximum deformation, maximum surface pressure, and time to reach these maximum values for viscoelastic impacts.

Method	$\phi_1(t)$ MPa	K MPa	α_m mm	Time to reach α_m ms	q_m MPa	Time to reach q_m ms
*Dynamic finite-element	$3.91\ e^{-203\,t}$	13.5	1.34	1.80	1.17	1.60
Rumsey and Fridley	$3.91\ e^{-203\,t}$	13.5	1.33	2.00	1.32	1.60
Hamann	†	†	1.32	2.00	1.24	1.50

*Time increment used = 0.01 ms

†Uniaxial relaxation function $\phi(t) = 11.03\ e^{-203t}$ MPa and a Poisson's ratio of 0.41 were used (Rumsey and Fridley, 1977).

$$\overline{\phi_1} = \frac{\frac{2K}{s}\left(\sum_{i=1}^{n} \frac{E_i}{s+\alpha_i}\right)}{\frac{6K}{s} - \frac{2}{3}\left(\sum_{i=1}^{n} \frac{E_i}{s+\alpha_i}\right)} \qquad [48]$$

where K is the elastic bulk modulus.

We developed a program by using an IMSL routine "FLINV" to invert equation [48] from the s-domain to the time-domain (Chen, 1983; and Crump, 1976). Thus, values of ϕ_1 at discrete points of time were obtained. A numerical method (Gil, 1982) was then used to fit a Maxwell model to the ϕ_1 values. Thus, ϕ_1 may be expressed as

$$\phi_1(t) = \sum_{m=1}^{M} G_m e^{-\beta_m t} \qquad [49]$$

This is the same as equation [12].

Constants for the shear relaxation function, ϕ_1, obtained for Golden Delicious apple flesh are listed in Table 3. These data are averaged values. The constants for the uniaxial relaxation function, ϕ, are listed in Table 4.

$$\phi(t) = \frac{\sigma(t)}{\varepsilon_o} \sum_{i=1}^{n} E_i e^{-\alpha_1 t} \qquad [50]$$

Note especially that constants determining the relaxation function developed here were measured at high-strain rate loadings and have multiple terms (Table 3) whereas the function given by Hamann (1970) has only one term. These features make the material property, ϕ_1, more appropriate to describe impact loadings, especially at the initial stage of impact.

The material properties in Table 3 were used in finite-element calculations

Table 3. Averaged constants for shear relaxation function, ϕ_1, for Golden Delicious apple flesh. $\phi_1 = \Sigma G_i (\exp(-\beta_i))$.

Impact Velocity m/s	G_1 MPa	G_2 MPa	G_3 MPa	G_4 MPa	β_1 s^{-1}	β_2 s^{-1}	β_3 s^{-1}	β_4 s^{-1}	K* MPa
0.7	0.636	0.111	0.208	0.099	.000347	.0409	1.121	35.26	1.756
1.2	0.710	0.134	0.265	0.119	.000380	.0420	1.633	41.30	2.047

*K is evaluated at initial time t=0, with Poisson's ratio of 0.25, i.e., $K = \Sigma E_i/(3(1-2\nu))$.

Table 4. Averaged constants for uniaxial relaxation function, ϕ, for Golden Delicious apple flesh. $\phi = \Sigma E_i (\exp(-\alpha_i t))$.

Impact Velocity m/sec	E_1 MPa	E_2 MPa	E_3 MPa	E_4 MPa	α_1 s^{-1}	α_2 s^{-1}	α_3 s^{-1}	α_4 s^{-1}
0.7	1.703	0.258	0.461	0.212	.000311	.0401	1.075	34.49
1.2	1.908	0.319	0.589	0.255	.000339	.0413	1.569	40.66

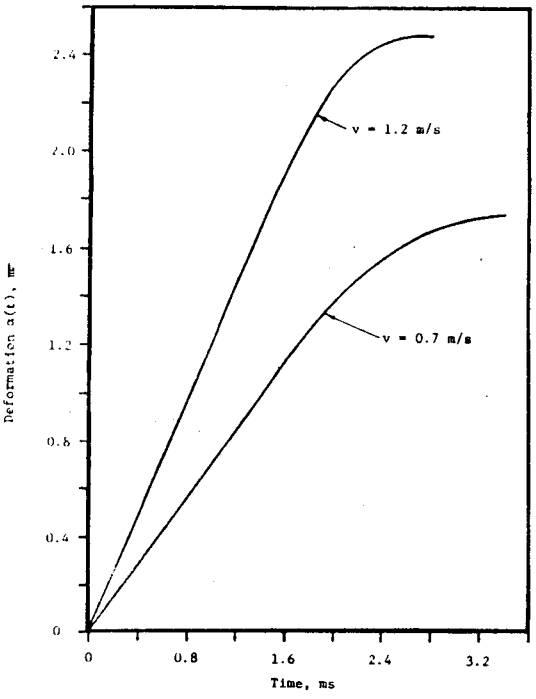

Fig. 5. The effect of impact velocity on deformation for viscoelastic impact of an apple on a rigid plate.

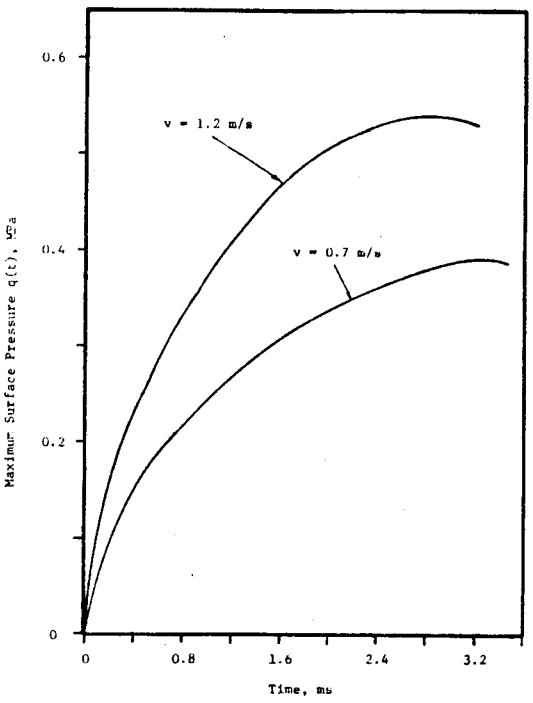

Fig. 6. Effect of impact velocity on maximum surface pressure for viscoelastic impact of an apple on a rigid plate.

for the impacts of apples, with radius of 0.035 m and density of 790 Kg/m^3, on a rigid plate at impact velocities of 0.7 and 1.2 m/s respecitvely. The deformations and surface pressures are shown in Figures 5 and 6. These results show that apples with impact velocity of 1.2 m/s took less time to reach maximum deformation and maximum surface pressure than apples with impact velocity of 0.7 m/s. Note also that at an impact velocity of 0.7 m/s, maximum surface pressure occurred about $2x10^{-4}$ seconds before maximum deformation. Whereas, at an impact velocity of 1.2 m/s, both occurred at about the same time.

Conclusions

The dynamic finite-element procedure developed in this paper proved successful in predicting the stress distribution in viscoelastic fruit during impact. This procedure predicts lower maximum surface pressure at the contact region than quasi-static methods. The maximum surface pressure may occur prior to the maximum deformation for viscoelastic impact, however, both occur at the same time for elastic impact. Further study is needed to correlate the results of this study with those of material-failure studies.

References

1. Bathe, K.J. and E. L. Wilson. 1976. Numerical methods in finite element analysis. Prentice-Hall, Inc., Englewood Cliffs, New Jersey.
2. Bathe, K.J. 1982. Finite element procedures in engineering analysis. Prentice-Hall, Inc., Englewood Cliffs, New Jersey.
3 Chen P. and S. Chen. 1986. Stress-relaxation functions of apples under high loading rates. Transactions of the ASAE 29(6):

1754-1759.
4. Chen, P. and S. Chen. 1984. Viscoelastic response of fruits to high strain rates. ASAE Paper No. 84-3555, ASAE, St. Joseph, Mich. 49085.
5. Chen, P. and R.B. Fridley. 1972. Analytical method for determining viscoelastic constants of agricultural materials. TRANSACTIONS of the ASAE 15(6): 1103-1106.
6. Chen, P., S. Tang, and S. Chen. 1985. Instrument for testing the response of fruits to impact. ASAE Paper No. 85-3537, ASAE, St. Joseph, MI 49085.
7. Chen, S., P. Chen, and L. R. Herrmann. 1984. Analysis of stresses in fruit during an impact. ASAE Paper No. 84-3554, ASAE, St. Joseph, MI 49085.
8. Chen, S. 1985. Engineering Analysis of viscoelastic response of fruits to impacts. Unpublished Ph. D. dissertation. University of California, Davis.
9. Chen, S. 1983. User's manual for program ILTRX, numerical inversion of Laplace transform of shear relaxation function. Department of Agricultural Engineering, University of California, Davis.
10. Clough, R.W. and J. Penzien. 1975. Dynamics of structures. McGraw-Hill Book Co., New York.
11. Crump, K.S. 1976. Numerical inversion of Laplace transforms using a Fourier series approximation. JACM 23(1): 89-96.
12. Gil, J. 1982. A numerical method for determining viscoelastic constants in agricultural materials. Unpublished M.S. Thesis, Department of Agricultural Engineering, University of California, Davis.
13. Goldsmith, W. 1960. Impact, theory and physical behavior of colliding solids. Edward Arnold Publishers, Ltd., London.
14. Hamann, D.D. 1969. Dynamic mechanical properties of apple flesh. TRANSACTIONS of the ASAE 12(1): 170-174.
15. Hamann, D.D. 1970. Analysis of stress during impact of furuit considered to be viscoelastic. TRANSACTIONS of the ASAE 13(6): 893-899.
16. Herrmann, L.R. and F.E. Peterson. 1968. A numerical procedure for viscoelastic stress analysis. Aerojet-General Report, Aerojet-General Corporation, Sacramento, California.
17. Herrmann, L.R. 1973. User's manual for viscoelastic analysis for 2-D solids program. Dept. of Civil Engr., University of California, Davis, California.
18. Horsfield, B.C., R.B. Fridley and L.L. Claypool. 1972. Application of theory of elasticity to the design of fruit harvesting and handling equipment for minimum bruising. TRANSACTIONS of the ASAE 14(4): 746-750.
19. Lapidus, L. and G.F. Pinder. 1982. Numerical solution of partial differential equations in science and engineering. John Wiley & Sons, New York.
20. Mohsenin, N.N. 1986. Physical properties of plant and animal materials. 2nd ed. Gordon and Breach Science Publishers, NY.
21. Manor, A.N. 1978. Critical analysis of the mechanics of fruit damage under impact conditions. Unpublished Ph.D. Thesis, Department of Agricultural Engineering, The Pennsylvania State University.
22. Moreland, L.W. and E.H. Lee. 1960. Stress analysis for linear viscoelastic materials with temperature variation. Transactions of the Society for Rheology. 4: 233-263.
23. Rumsey, T.R. and R.B. Fridley. 1977. Analysis of viscoelastic contact stresses in agricultural products using a finite element method. TRANSACTIONS of the ASAE 20(1): 162-167, 171.
24. Rumsey, T.R. and R.B. Fridley. 1977. A method for determining the shear relaxation function of agricultural materials. TRANSACTIONS of the ASAE 20(2): 386-389, 392.
25. Timoshenko, S.P. and J.N. Goodier. 1951. Theory of elasticity. McGraw-Hill, NY.
26. Yang, W.H. 1966. The contact problem for viscoelastic bodies. TRANSACTIONS of ASME, Journal of Applied Mechanics 33(4): 395-401.
27. Zienkiewicz, O.C. 1977. The finite element method. 3rd ed. McGraw-Hill Book Co., New York.